Journal of Applied Polymer Science

Surface and wetting characteristics of textured bisphenol-A based polycarbonate surfaces: Acetone-induced crystallization texturing methods

Ahmed Owais,[1] Mazen M. Khaled,[2] Bekir S. Yilbas,[3] Numan Abu-Dheir,[3] Kripa K. Varanasi,[4] Kamal Y. Toumi[4]

[1]Renewable Energy Science and Engineering Department, Faculty of Postgraduate Studies for Advanced Sciences (PSAS), Beni-Suef University, Beni-Suef 62511, Egypt

[2]Chemistry Department, King Fahd University of Petroleum and Minerals, Dhahran 31261, Saudi Arabia

[3]Mechanical Engineering Department, King Fahd University of Petroleum and Minerals, Dhahran 31261, Saudi Arabia

[4]Mechanical Engineering Department, Massachusetts Institute of Technology, Cambridge Massachusetts 02139-4307

Correspondence to: M. M. Khaled (E-mail: mkhaled@kfupm.edu.sa)

ABSTRACT: Polycarbonate (PC) sheet is a promising material for facile patterning to induce hydrophobic self-cleaning and dust repelling properties for photovoltaic panels' protection. An investigation to texture PC sheet surfaces to develop a self-cleaning structure using solvent induced-crystallization is carried out using acetone. Acetone is applied in both liquid and vapor states to generate a hierarchically structured surface that would improve its contacts angle and therefore improve hydrophobicity. The surface texture is investigated and characterized using atomic force microscopy, contact angle technique (Goniometer), optical microscopy, ultraviolet-visible spectroscopy (UV–vis) and Fourier transform infrared spectroscopy. The findings revealed that the liquid acetone-induced crystallization of PC surface leads to a hierarchal and hydrophobic surface with an average contact angle of 135° and average transmittance <2%. However, the acetone vapor induced-crystallization results in a slightly hydrophilic hierarchal textured surface with high transmittance; in which case, average contact angle of 89° and average transmittance of 69% are achieved. © 2015 Wiley Periodicals, Inc. J. Appl. Polym. Sci. **2016**, *133*, 43074.

KEYWORDS: crystallization; hydrophobicity; polycarbonate sheet; solar cells; surface texturing

Received 29 April 2015; accepted 21 October 2015

DOI: 10.1002/app.43074

INTRODUCTION

In the last decade, several studies have been performed to develop the different techniques to design and produce hydrophobic surfaces by controlling the surface topography and chemistry.[1,2] Accumulation of dust,[3] as well as snow,[4] over the polycarbonate (PC) sheet surface becomes problematic and adversely affects the photovoltaic (PV) efficiency owing to lowering the transmittance of the solar radiation reaching the active area of the PV panel.[5] Lotus leaf has gained the main the focus of the scientists who are interested in that field of research because its surface is rough and hydrophobic, contact angle >150° and sliding angle <10°.[6] Several crop plants also have the same characteristics like the Lotus leave, for example, Brassica, Alchemellia, and Lupinus.[7] Mimicking the nature and generating surface hydrophobicity improves the performance of the PV devices through minimizing the dust accummulation at the surface. One of the promising materials to be modified to develop hydrophobicity is the PC sheet. PC sheet is one of the protective covers for PV panels due to its high mechanical flexibility and low density. It was reported that surface texturing of PC sheet at micro/nano scales resulted in a hydrophobic texture.[8] Texturing the hydrophobic surfaces enhances the non-wetting properties by increasing the trapped air between the surface texture posts. This, in turn, leads to a superhydrophobic behavior of the textured surface, since liquid droplets lay on the air pockets. Surface texturing and modification of polymers toward achieving surface hydrophobicity and characterization were central interest by the researchers.[9–12] This is mainly because of easiness of surface modification and processing of polymers to achieve hydrophobic characteristics.

Additional Supporting Information may be found in the online version of this article.

PCs are considered as an organic polymeric material with two subclasses, aliphatic and aromatic. The bisphenol A [2,2-bis(p-hydroxyphenyl) propane]-based PCs has interesting characteristics like high toughness, high transparency, high heat capability, low water absorbability, low synthesis cost, and ease of decoration; therefore, industrially, they are considered the most important polymers.[13,14] Synthesis of PCs includes four different methods: (**i**) interfacial synthesis, (**ii**) transesterification, (**iii**) oxidative carboxylation, and (**iv**) synthesis using CO_2. Polymer crystallization is a kinetic process, in which molecular or atomic rearrangement process takes place to achieve stable orientations. Semicrystalline polymers have many industrial applications, so scientists have directed their attentions along the last 60 years on studying this category of polymers. The crystallization process involves three main steps: (**i**) Initiation of crystallization, (**ii**) Primary crystallization, and (**iii**) Secondary crystallization.[15] The Hildebrand solubility parameters of both the PC and the acetone are almost the same, 20.1 and 20.3 H, respectively,[16,17] so that they are completely miscible.[18] The interaction between the PC and acetone is used so as to texture the PC surface and form a hierarchical structure.[8] This is a crystallization reaction, where physical changes occur at the surface of the PC due to the phase-phase interaction between the PC surface and the acetone. This physical change leads to creating the hierarchical surface pattern with a certain roughness. The semicrystalline polymers have higher chemical resistance, while amorphous polymers have a lower one. One more characteristic for the amorphous polymers is the high chain mobility, which induces its crystallization through a very slow process.[19] Polymer crystallization process can be induced either thermally or by using organic or inorganic solvents.[20,21] Liang *et al.*[22] used diallyl-orthophtalate as a solvent to induce the PC crystallization process, in the presence of plasticizers. Turska *et al.*[23] treated the PC samples thermally, by heating till 190°C for seven days, in order to get a low degree of crystallization, which is 23% on average. It was demonstrated that the best organic solvent which can induce the PC crystallization process efficiently is the acetone.[24,25]

Several other methods can be used to texture the PC surfaces,[26] and acetone crystallization is the most direct, economic and scalable method. The critical problem of increasing roughness is the light reflectance from the rough-surface and, as a consequence, the decrease of the rough-surface light-transmittance; therefore controlling the surface roughing process should be taken into consideration.[27] Generally, several types of rough surfaces can be designed by many techniques; every technique has its own characteristics, advantages and disadvantages,[28] for example, photolithography, template method, laser etching, . . .etc. Bruynooghe *et al.* enhanced the light transmittance of the sheet surface by coating it with an antireflective material (containing expensive MgF_2 material) and, subsequently, with a hydrophobic and oleophobic coating material. They achieved a contact angle of 110° after coating with 0.14% reflectance at incident angle of 78° in the spectral region 400–680 nm.[29] Wang *et al.* achieved a superhydrophobic (CA of ~164) surface with an anticorrosion property by using expensive two fluorinated compounds, polyvinylidene fluoride and fluorinated ethylene propylene, in addition to carbon nanofibers, which causes surface opaque.[30] Nakajima *et al.* designed boehmite-TiO_2 films, with varied TiO_2 compositions, and a following (heptadecafluorodecyl) trimethoxysilane (FAS-17) coating, which was used as superhydrophobic coating materials. However, it was also reported that TiO_2-based coatings could be affected by UV light, especially at higher TiO_2 compositions, leading to hydrophobicity drop due to the photocatalytic effect (strong oxidation power under UV light) of the TiO_2.[27] De Oliveira *et al.* casted a bisphenol-A PC film, with different molar mass, and exposed it to acetone vapor-saturated environment for one and two days. The study deduced that there was a direct relationship between the polymer molar mass, the melting enthalpy, the dimensions of the formed spherules and the degree of crystallization.[19] Liu *et al.* studied the effect of PC thickness on the acetone transport kinetics within the polymer sheets.[31] Varanasi group has used of liquid acetone-induced PC crystallization to create superhydrophobic surfaces. They achieved a high contact angle with low contact angle hysteresis between the textured, crystallized PC surface and a water droplet.[8]

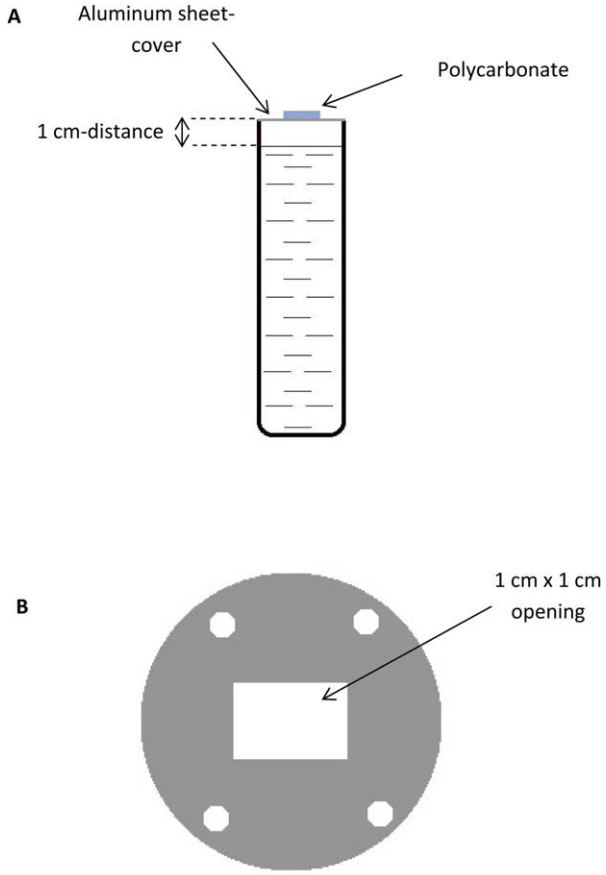

Figure 1. (A) The designed setup for the liquid-vapor interface method (lateral view). (B) 1 × 1 cm^2 vapor-outlet. [Color figure can be viewed in the online issue, which is available at wileyonlinelibrary.com.]

In this study, surface texturing the PC sheet is carried out using two different single-step methodologies by varying the physical state of the acetone. Acetone is used in its liquid state to induce crystallization of the smooth untreated PC sheet surface by

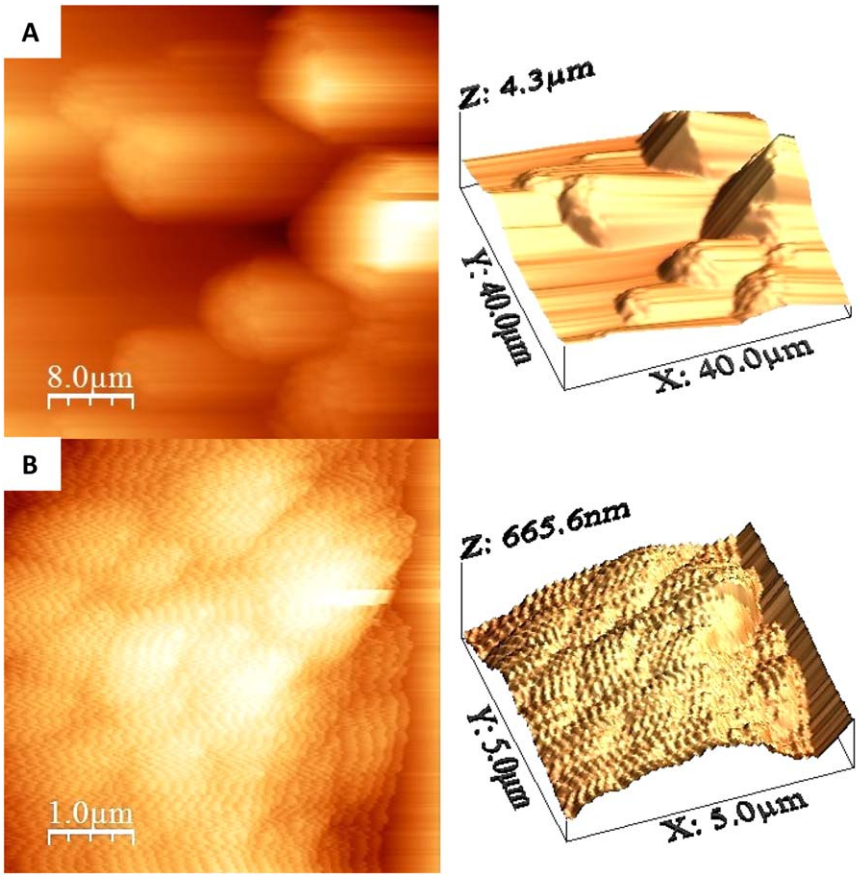

Figure 2. 2D and 3D AFM micrographs for a textured PC surface by immersion in pure liquid acetone for 10 min at: (A) 40 μm scale. (B) 5 μm scale. [Color figure can be viewed in the online issue, which is available at wileyonlinelibrary.com.]

immersion process. Additionally, smooth untreated PC surface is crystallized by exposure to acetone vapor and the resulting textured surfaces are investigated and compared. The tribology, hydrophobicity, transmittance, and surface chemistry are characterized by using several analytical tools. An atomic force microscope (AFM) and an optical microscope were used to analyze the PC sheet surface topography. Goniometer is used to measure the contact angle of a sessile DI water droplet of 0.1 μL over the PC sheet surface. Ultraviolet-visible spectroscopy (UV–vis) and Fourier-Transform IR spectrophotometers are used to measure transmittance and surface chemical structure of the PC sheet, respectively.

EXPERIMENTAL

PCs sheets, of thickness 1.6 mm and produced by Makrolon from Bayer Material Science, were obtained from Sheffield Plastics (Sheffield, MA). Liquid acetone, from Sigma Aldrich (purity $\geq$ 99.5%, b.p: 56°C, MW: 58.08 and v.p: 184 mmHg at 20°C), was used for crystallization process. For the texturing process with the liquid acetone PC sheets were immersed for 10 min at room temperature (18°C).[8] In addition, the PC sheet was crystallized and textured by the exposure to acetone vapor at the room temperature (18°C) for an average of 8 h. A 1 cm-distance was maintained between the liquid phase (acetone) surface and the exposed PC surface during the process.

AFM/SPM (5100-Agilent technologies) was used for scan and characterizing the surface topography and roughness profile in contact mode. Image analysis was performed using software WSxM v5.0 Develop 6.2.[32] A silicon nitride probes tip was used with radius in the range of 20–60 nm and specified force constant (k) of 0.12 N/m manufactured by Brucker AFM Probes. Attenuated Total Reflection Fourier-Transform Infrared (ATR-FTIR) (Bruker Vertex 70) was used in the identification of different functional groups that are present on the surface before and after the texturing process. UV–vis spectrophotometer (PerkinElmer) was used to measure the transmittance of the PC sheet before and after the patterning process. X-ray Diffraction (XRD) was used to analyze the degree of surface crystallinity with scanning angle 2θ and scanning range 5°–80°. Goniometer (KYOWA DM-701) is used to determine the degree of both the hydrophilicity and the hydrophobicity of the surface by measuring the static contact angles between a deionized water droplet (of 0.4–5 μL volume) and the surface. Figure 1 shows the experimental setup for the crystallization process.

RESULTS AND DISCUSSION

Surface texturing of PC sheet is achieved using the crystallization process through direct immersion in liquid acetone and through exposure to acetone vapor. Morphological and hydrophobic characteristics of the surface are assessed via analytical tools.

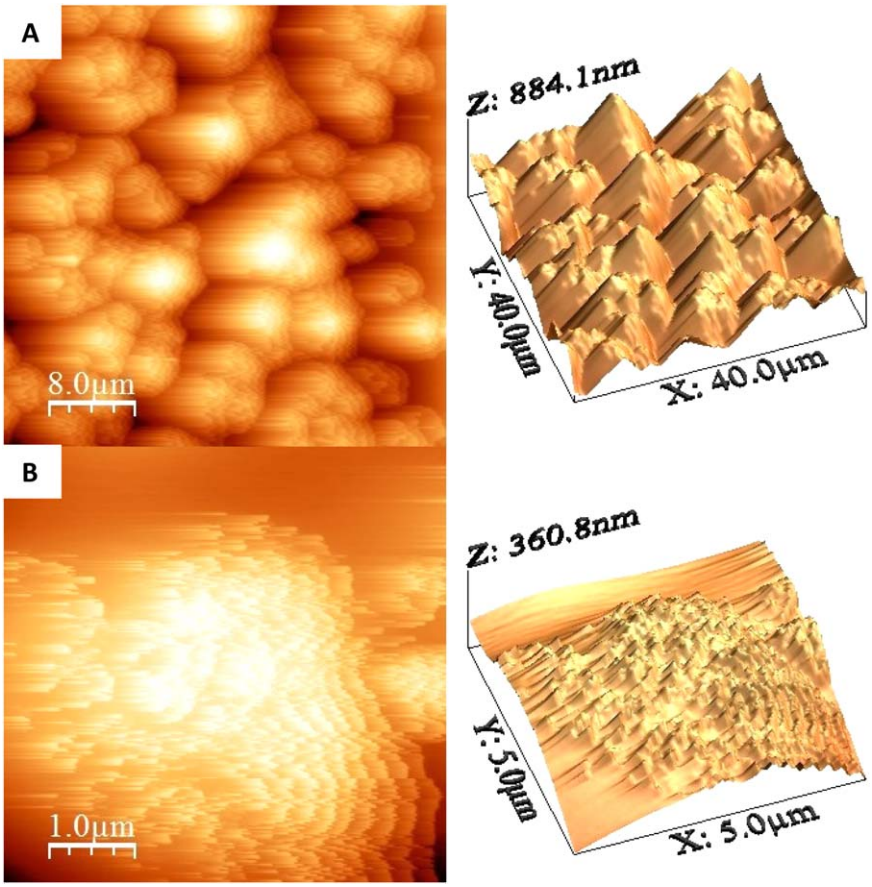

Figure 3. 2D and 3D AFM micrographs for a textured PC surface by exposure to pure acetone vapor for 24 h at: (A) 40 μm scale. (B) 5 μm scale. [Color figure can be viewed in the online issue, which is available at wileyonlinelibrary.com.]

Analysis of several AFM scans for different areas of the textured PC sheet surfaces shows the development of specific and unique features under different conditions. Figure 2 shows an AFM micrograph, illustrating the appearance of a new surface texture after immersion in acetone. Immersion of PC surface in liquid acetone resulted in large spherules appear over the surface after immersing the sample for 10 min, Figure 2(A). The average width of the spherules observed is in the range of 12 μm. At lower scan widths, Figure 2(B), the surfaces of the spherules become more apparent and the sharp textures on top of it can be clearly observed. It can be noticed that the surface of the spherule does not have uniform texture, in other words, the spherule's surface becomes hilly; and this hilly surface is full of a grass-like textures.

The textured surface with acetone vapor shows more fine and detailed structures, Figure 3(A), with a scanning scale of 40 μm, shows well-detailed spherules after exposure of the smooth PC sample to the acetone vapor. The average width of the spherules observed, in the figure, is in the range of 8 μm, compared with 12 μm for average width of spherules generated due to immersion in liquid acetone. From Figure 3(B), it can be inferred that the hills display is not evident and mainly the grass-like textures appear at the spherules' surfaces.

The study is extended to include the topology of the textured surfaces by using different line profiles of the AFM micrographs. For the textured PC surface by immersion in acetone liquid, Figure 4(A), the typical height of the spherules may be reported as 1.8 μm. The width of the middle spherule is in the range of 13 μm. In Figure 4(B), a distinctive line profile of the single spherule appears. The spherule contains three small elevations over its surface, each elevation is textured. This is consistent with the observation of the hilly surface and the grass-like hills, which is pointed out earlier in the description of Figure 2(A). In Figure 4(C), the height of the spherules is in the range of 375 nm, whereas the width of the left spherule lies within the range of 13.5 μm. In Figure 4(D), a distinctive line profile of the AFM micrograph of a single spherule's surface appears. The spherule contains grass-like structure over its surface; this grass resembles the surface texture. AFM and surface line profile micrographs of the untreated PC sheet surface can be found in the Supporting Information Figures S1 and S2, which assures the absence of any texture on the surface. The generation of the spherules is related back to a molecular or atomic rearrangement process takes place in order to achieve stable orientations, which is termed a crystallization process.

The liquid induced-crystallization process of PC surface process, by immersion in liquid acetone, leads to a molecular rearrangement on the surface of the PC sheet and to several microns in depth, leading to generation of spherule-like crystalline structures and creating a hierarchal textured surface of high

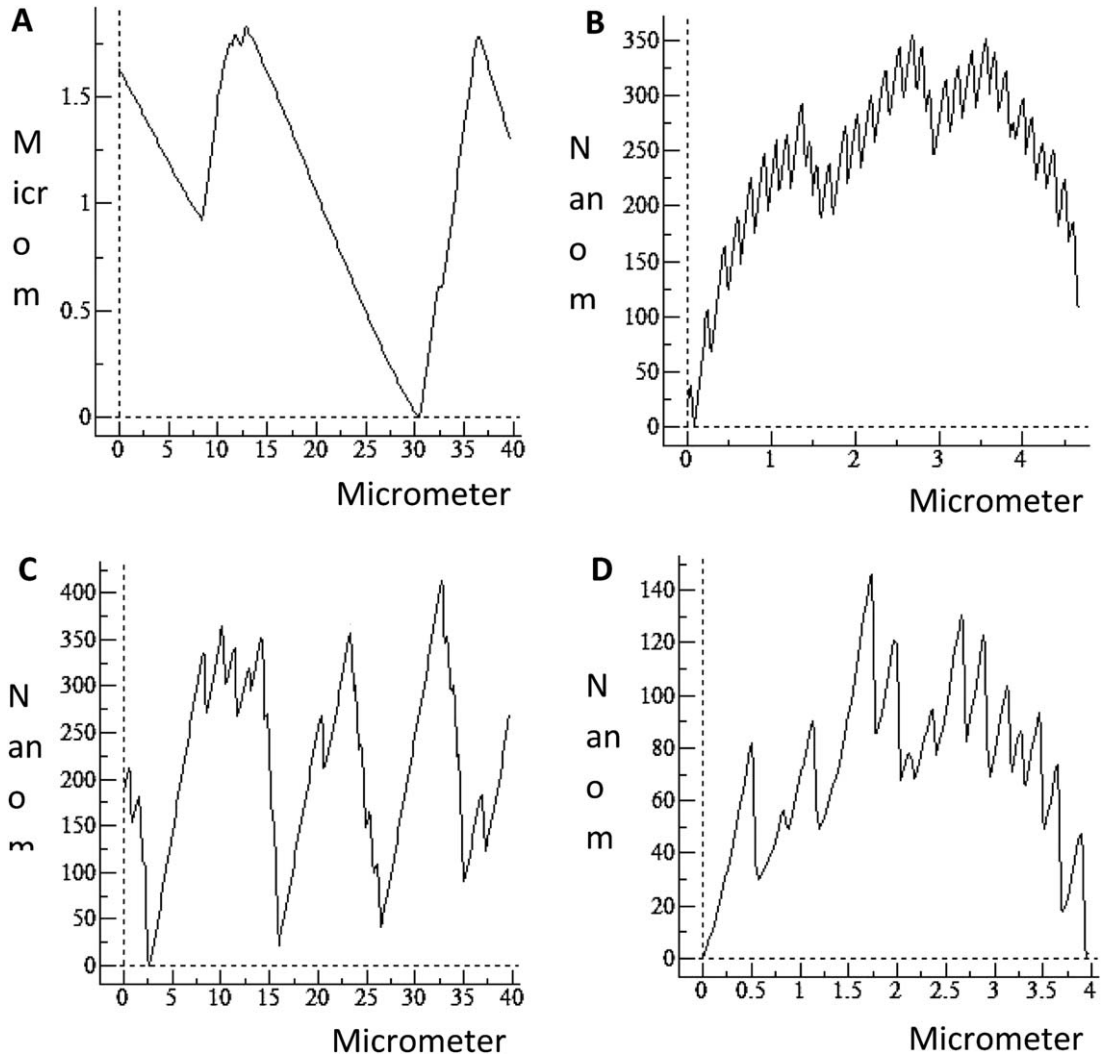

Figure 4. (A) 40 μm scale and (B) 5 μm scale line profiles of the AFM micrographs for a textured PC surface by immersion in pure liquid acetone for 10 min. (C) 40 μm scale and (D) 5 μm scale line profiles of the AFM micrographs for a textured PC surface by exposure to pure acetone vapor for 24 h. The four profiles prove the formation of the hierarchical structure after the solvent-induced crystallization process. Line profiles A and C (at 40 μm) show different textured surfaces in micro (for A) and nano (for C) scales due to surface crystallization by treatment with acetone liquid and vapor, respectively. Line profiles B and D show different textured surfaces with dense (for B) and sprinkled (for D) pillars due to surface crystallization by treatment with acetone liquid and vapor, respectively.

roughness. This can be related to the hydrostatic pressure that is applied on the immersed PC surface in the liquid acetone. However, the textured PC sheet surfaces due to vapor-induced crystallization have small crystals owing to the high nucleation density. Despite of the enlargement of the crystals grain-sizes due to increasing the exposure time of the PC sheet surface to the acetone vapor, however, reaching large crystals with perfectness stills arduous.[33]

The size of the generated spherules and the polymer surface degree of crystallinity is directly proportional to the depth to which acetone diffuses. Furthermore, pores formation takes place if the layer depth is larger than the width of the spherule; however, incomplete spherule coverage results in case of less layer depth than the spherule dimensions.

For the solid-vapor method of polymer crystallization, the acetone vapor condenses over the PC surface. Therefore, the PC becomes in contact with, only, 1 mL of acetone on average. As a consequence, the mass transfer in this case becomes considerably lower than that in case of immersing the surface in the liquid acetone. Mass transfer, which is a driving-force dependent, affects the diffusion process significantly. The mass transfer equation between two phases is[34]:

$$N_A = k\ a\ \Delta C_A \quad (1)$$

where N_A: the mass transfer rate of component A, k: the mass transfer coefficient, a: the transfer area, ΔC_A: the concentration driving force. The driving force is the result of the difference between the concentration of the liquid in the bulk and the concentration of the liquid in the formed boundary-film interface. Therefore, the concentration of the liquid in the bulk is larger, in case of the immersion in liquid acetone, than that in case of exposing the polymer surface to acetone vapor.

Table I. Surface Roughness Data of PC Sheet Samples, Obtained from AFM Study

Image scale (μm)	RMS values (nm)		
	Untreated PC	Solid-vapor PC	Solid-liquid PC
40	23.99 ± 1.10	131.19 ± 1.32	610 ± 6.1
20	11.52 ± 0.55	135.61 ± 1,35	543.1 ± 5.2
10	5.26 ± 0.22	97.65 ± 0.98	250 ± 2.4
5	2.44 ± 0.11	65.83 ± 0.66	108.4 ± 1.1
1	0.81 ± 0.04	18.36 ± 0.20	31.1 ± 0.3
0.5	0.73 ± 0.04	15.21 ± 0.15	27.6 ± 0.3

Scale (μm)	Ra values (nm)		
	Untreated PC	Solid-Vapor PC	Solid-Liquid PC
40	18.85 ± 0.19	104.27 ± 1.11	460 ± 4.61
20	9.27 ± 0.91	109.57 ± 1.11	407 ± 4.11
10	4.19 ± 0.42	76.78 ± 0.81	210 ± 2.12
5	1.9 ± 0.02	55.12 ± 0.6	87.61 ± 0.76
1	0.64 ± 0.01	15.0 ± 0.15	25.01 ± 0.25
0.5	0.58 ± 0.01	11.39 ± 0.12	22.74 ± 0.21

Consequently, deeper diffusion and larger crystals take place in the former case.[17] In case of exposing the PC surface to the acetone vapor, the gravitational force has an effect on reducing the diffusion extent, but its effect is omitted in the present study and it is considered to be small.

Roughness of the different crystallized surfaces can be determined, using the AFM. The study gives the roughness of the PC surfaces (smooth, textured by immersion in liquid acetone and textured by exposure to acetone vapor) much concentration because it is one of the parameters that are responsible for the hydrophilicity or the hydrophobicity of the surface. Table I gives the surface roughness data obtained from AFM study. It is clear from the values of both the RMS and Ra that the textured PC surface by immersion in pure liquid acetone has the highest roughness, even far higher than the roughness of the textured PC surface by exposure to pure acetone vapor. This allows deep diffusion of the acetone liquid within the polymer layer, leading to complete-crystals coverage, pores formation and as a consequence, high roughness in a very short duration. Both the weak gas pressure and the low mass transfer lead to a relatively shallow diffusion of acetone in the acetone vapor case, and hence, the incomplete coverage of crystals and low roughness values occurred, despite the long vapor treatment durations.

Figure 5 shows transmittance data for smooth and textured PC sheet surfaces including immersion and vapor induced texturing. Textured, rough PC sheets, due to immersion in liquid acetone for 10 minutes, exposed to UV and visible spectra, starting from 400 to 800 nm to measure their transmittance values. The average transmittance of this surface is as low as 2%, referring to an opaque surface. Textured, rough PC sheets, due to exposure to acetone vapor, also exposed to UV–vis spectra, 400 to 800 nm, to measure the transmittance. The PC sheet surface was exposed to pure acetone vapor for 30 min. The average transmittance of this sample is 69.42%. Transmittance also reduces due to the reflection process of the incident radiation. The reflection process is a certain result of the light scattering from the textured PC surface. Rayleigh scattering is applied on the vapor textured surfaces because the spherules dimensions are slightly smaller or almost equal to the wavelengths of the incident light, visible light 400–800 nm according to Rayleigh theory.[35]

$$I \propto d^6$$

This relationship illustrates how sensitive the diameter of the texture is, in case of the presence of smaller texture than the incident light wavelength. Any small change in the diameter value results in magnifying the intensity of the scattered light by 6 times. This explains the reduction in the average transmittance values, which accompanies the increase in the spherule width due to either long exposure duration to the acetone vapor or immersing the sample in liquid acetone for extended period.

In relation to the surface hydrophobicity, two states can describe the behavior of the textured surface towards the water droplet, with which it is in contact: (**i**) Cassie-Baxter's state and (**ii**) Wenzel's state. For the hydrophobic surfaces (contact angle $\theta > 90°$), Cassie-Baxter state is applied, whose equation[36] is:

$$\cos\theta_{cb} = \phi_s(\cos\theta_y + 1) - 1 \quad (2)$$

where θcb: the Cassie's (apparent) contact angle, $\theta cb > 90°$, θy: the Young's contact angle (contact angle of the corresponding smooth surface) and φs: the solid fraction which is in contact with the water droplet. For calculating the value of φs for the single textured hydrophobic surface:

$$\phi_s = \frac{\cos\theta_{cb} + 1}{\cos\theta_y + 1} \quad (3)$$

Wenzel's state is applicable for the hydrophilic textured surfaces, whose apparent contact angles are lower than the right angle ($\theta < 90°$). Wenzel's equation is as the following[37]:

$$\cos\theta_w = r\cos\theta_y \quad (4)$$

where θw: the Wenzel's (apparent) contact angle, $\theta w < 90°$, θy:

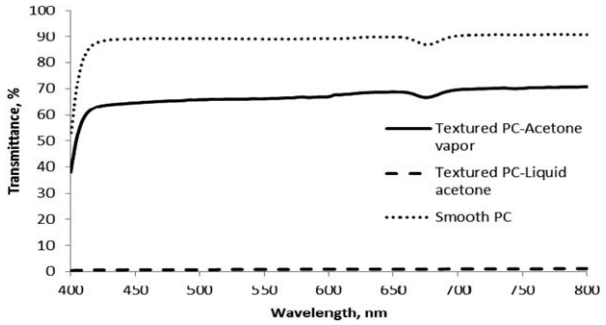

Figure 5. Visible spectra of smooth, liquid acetone-textured and vapor-acetone-textured PC sheet surfaces.

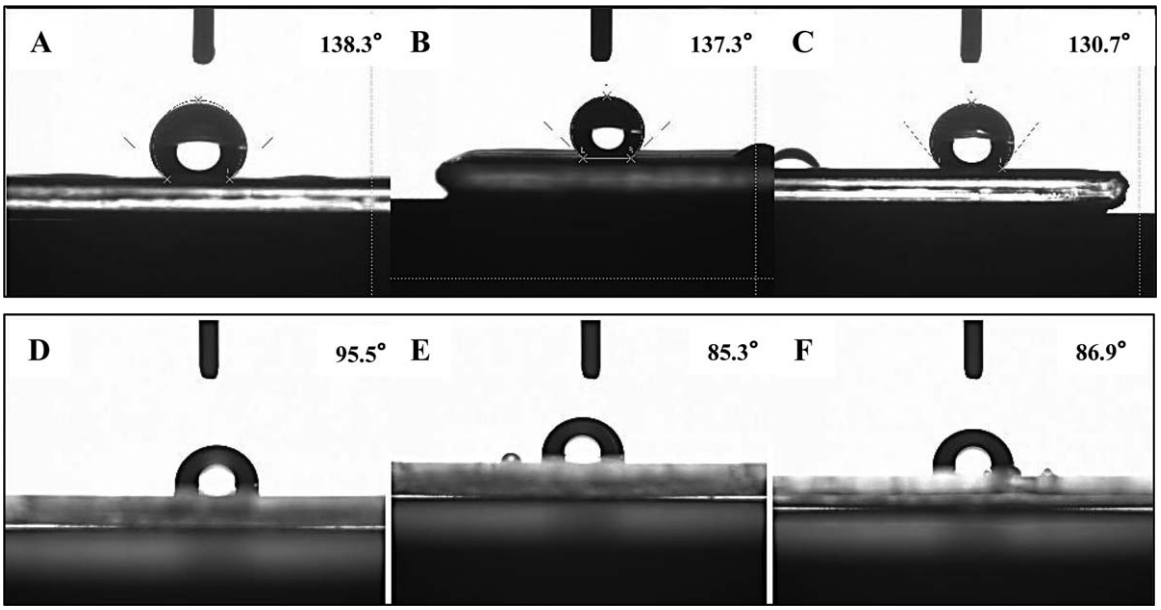

Figure 6. (A–C) CA of a textured PC sample by immersion in pure liquid acetone for 10 min. (D–F) CA of a textured PC sample by exposure to pure acetone vapor for 30 min.

the Young's contact angle (contact angle of the corresponding smooth surface) and r: the roughness ratio factor of the textured surface. For calculating the value of r for the single textured hydrophobic surface:

$$r = \frac{\cos\theta_w}{\cos\theta_y} \tag{5}$$

Contact angle of the patterned PC surface is measured, using a deionized water droplet over different spots on the textured surface and measured by using the Goniometer's camera. For the PC sheet immersed for 10 minutes, the contact angles of the three different areas over the surface are 138.3, 137.3, and 130.7°, Figure 6(A–C), respectively. For the PC sheet surface exposed to acetone vapor for 30 min, the contact angles of three different areas over the surface are 95.5, 85.3, and 86.9°, Figure 6(D–F), respectively. The average contact angle for this sample is 89.23°.

An optical microscope is used to examine the morphology of the immersed PC surface. The first phase can be characterized and the shape and growth of the generated spherules due to the crystallization process. Furthermore, the gaps or the distances between the spherules, where the crystallization process are absent to some extent, can be clearly observed. The scale bar of most of the images is 100 μm. For the PC sheet immersed in liquid acetone, Figure 7(A), the fused mature spherules can be well distinguished from the nonmature spherules that grow within the gaps. For the textured PC sheet surface due to exposure to acetone vapor, the spherules continue their growth and aggregations formation. In addition, it can be noticed that there is a fusion occurring between the adjacent grown spherules, Figure 7(B). The width of the single spherule is in the range of 5 μm. From the images of optical microscope, it can be generally inferred that the average spherules widths of the textured surfaces by the solid-liquid interface method of crystallization are

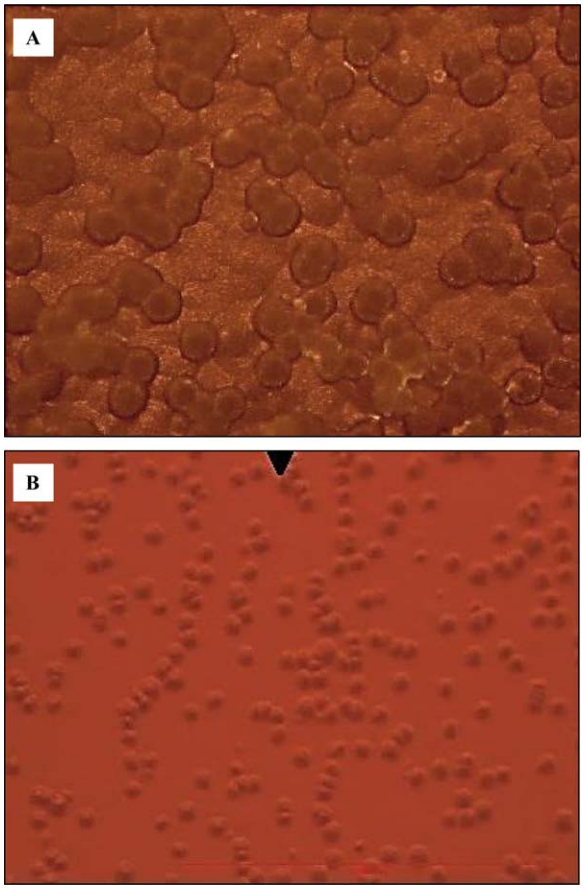

Figure 7. (A) Optical microscope image of a textured PC sample by immersion in pure liquid acetone for 10 min. (B) Optical microscope image of a textured PC sample by exposure to pure acetone vapor for 30 min. [Color figure can be viewed in the online issue, which is available at wileyonlinelibrary.com.]

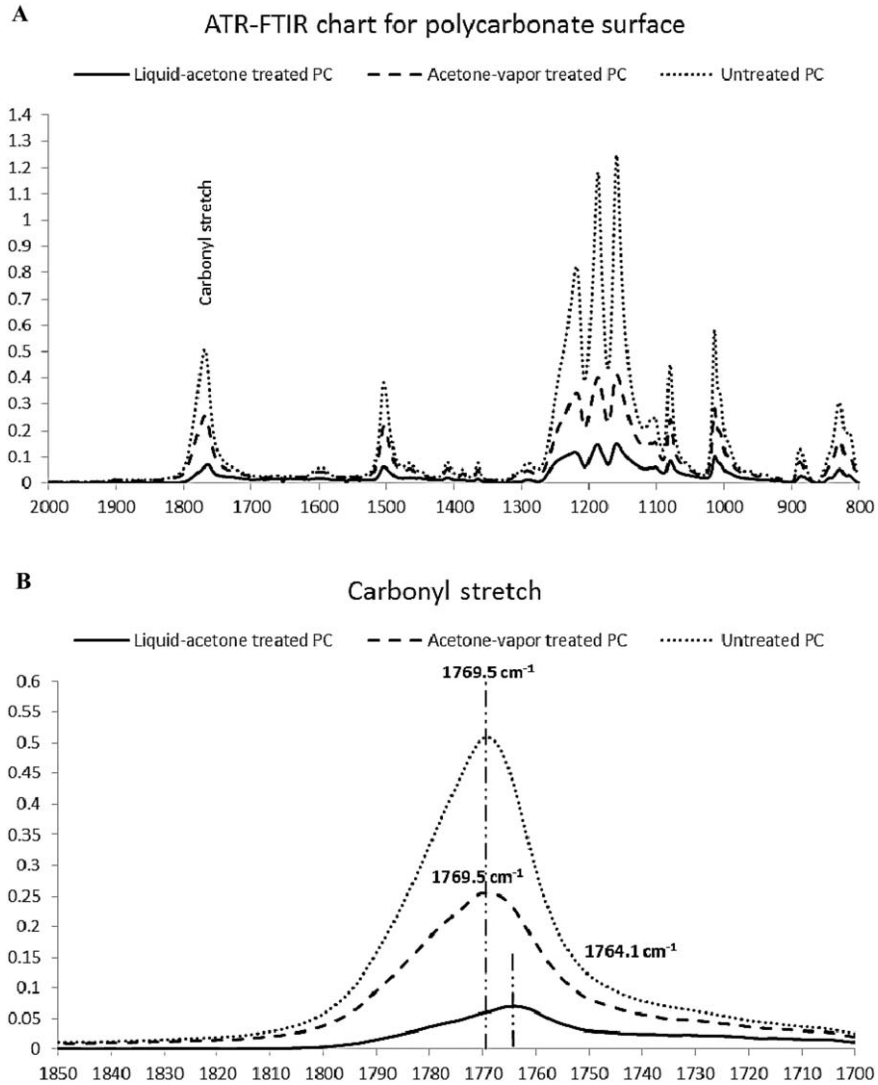

Figure 8. ATR-FTIR spectra of smooth, liquid acetone-textured and vapor-acetone-textured PC sheets surfaces. (A) whole spectra and (B) Carbonyl stretching mode peak.

totally larger than the widths of the spherules present over the textured surfaces by the solid-vapor interface method of crystallization. Furthermore, according to the line profiles of the AFM micrographs the gaps within the texture in the patterned PC samples by the solid-liquid interface method of crystallization are smaller in width than those present over the textured surfaces by the solid-vapor interface method of crystallization.

Attenuated Total Reflection Fourier-transform Infrared (ATR-FTIR) technique is used for detecting chemical, functional, side and terminal groups, which are present in a chemical compound through the detection of the different stretching and bending modes of the bonds, present in these groups. Figure 8(A) shows ATR-FTIR spectra of untreated smooth, vapor-acetone-textured, and liquid acetone-textured PC glass surfaces. The acetone treatment effect is observable at the wavelength at which the peak of carbonyl, C═O. Prior to exposure to acetone, the peak of carbonyl stretching mode is observed at 1769.5 cm^{-1}, Figure 8(B).

After exposure to acetone, an increase in crystallization noted by a shift in the wavenumber of the carbonyl group to 1764 cm^{-1},[31,38] Figure 8(B). Amorphous form of polymer gives a relatively higher degree of freedom to the polymers tail motion.[19] This the performance of stronger vibrations, in case of molecules or groups that have a dipole moment (asymmetric chemical structure).[39] This also allows chains motion and bonds vibrations in the crystalline phase, in which the molecules are tightly packed and consequently, the vibrations and motions are restricted.[19,40,41] This behavior indicates that the acetone interaction with the PC is a physical process because there is no new peak emerged after the treatment process.[31] XRD was used to verify the crystallization of the PC surface, Figure 9. However, CuKα ray penetrates a surface layer on the order of 600–900 μm.[42] Although penetration depth is greater than the expected thickness of the crystalline spherulitic layer, the sharpening of the XRD peaks for samples with more aggressive crystallization where liquid acetone is used, indicates an increase in the

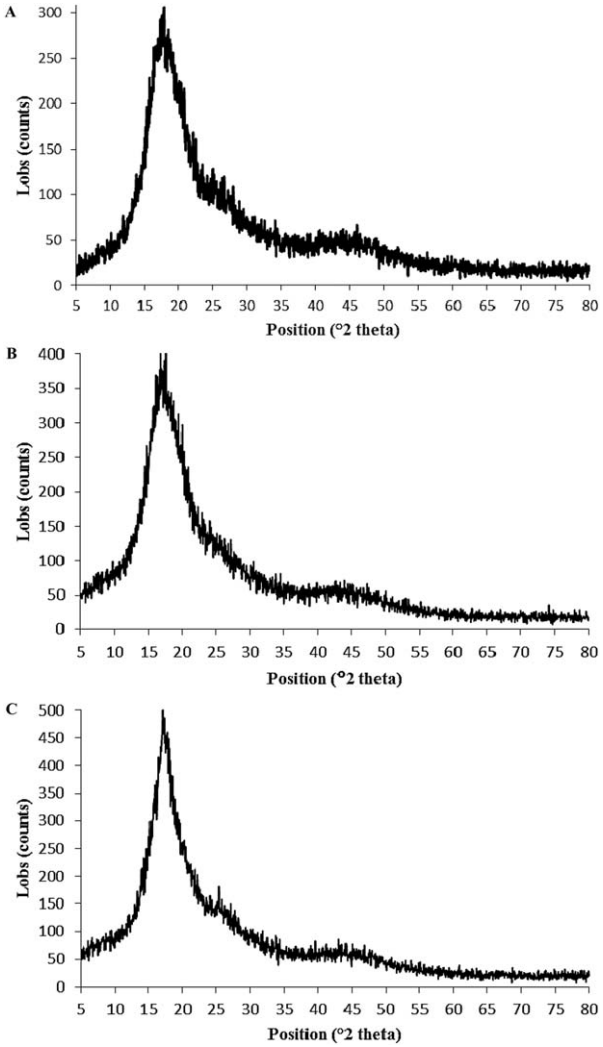

Figure 9. XRD data for (A) untreated PC sheet. (B) a textured PC sheet by immersion in pure liquid acetone for 10 min. (C) a textured PC sheet by exposure to pure acetone vapor for 30 min.

crystallinity of the total irradiated volume. Further, the narrowing of the peak width indicates an increase in the thickness of the crystalline layer.

CONCLUSIONS

Two methods of surface texturing are investigated for the solvent-induced crystallization process of a PC surface including liquid acetone and acetone vapor induced crystallization. AFM, Goniometer, optical microscope, UV–vis, and ATR-FTIR are used to characterize the textured PC sheet surfaces. It is found that textured PC sheet surface due to immersion in liquid acetone for 10 min shows formation of 13 μm-in width large spherules (crystals) and 1750 nm-in depth gaps over the surface which are responsible for the high contact angle of 135° and low visible-light transmittance, which is <2%. Cassie-Baxter state for hydrophobic surfaces is applicable and the resulted solid fraction value (φ_s) is 0.26, in agreement with the high apparent contact angle of the sample. For the textured PC sheet surface by exposure to acetone vapor for 30 min, AFM micrographs illustrate the presence of 5 μm-in width spherules and 360 nm-in depth gaps formation, which in turn results in decreasing hydrophobicity having 89° average apparent contact angle; however, surface transmittance is tremendously enhanced by 67% to reach 69%. Since the surface is wettable, the Wenzel state is applied and the value of the roughness ratio (r) is 0.13, which indicates the weak hydrophilicity state of the textured surface. ATR-FTIR and XRD data, by IR absorption peak shift and XRD 2θ-peak sharpness respectively, indicated the occurrence of the strong crystallization at the PC surface when induced with pure liquid acetone. In addition, the tremendous decrease in the IR absorbance chart peaks intensities is observed and the XRD 2θ peaks increase and sharpen.

ACKNOWLEDGMENTS

This project was funded by the National Plan for Science, Technology, and Innovation (MAARIFAH)—King Abdulaziz City for Science and Technology—through the Science and Technology Unit at King Fahd University of Petroleum and Minerals (KFUPM)—The Kingdom of Saudi Arabia, award number (11-ADV2134-04). The support from the Center of Excellence for Research Collaboration with MIT is also acknowledged for support through projects numbers MIT11111-11112. The authors also acknowledge the financial support from Materials Science and Nanotechnology Department at the Faculty of Postgraduate Studies for Advanced Sciences at Beni-Suef University, Egypt.

REFERENCES

1. Gao, L.; McCarthy, T. J. *J. Am. Chem. Soc.* **2006**, *128*, 9052.
2. Liu, H.; Wang, X.; Ji, H. *Appl. Surf. Sci.* **2014**, *288*, 341.
3. Said, S. A.; Walwil, H. M. *Sol. Energy* **2014**, *107*, 328.
4. Andrews, R. W.; Pollard, A.; Pearce, J. M. *Sol. Energy Mater. Sol. Cells* **2013**, *113*, 71.
5. Cecchetto, L.; Serenelli, L.; Agarwal, G.; Izzi, M.; Salza, E.; Tucci, M. *Sol. Energy Mater. Sol. Cells* **2013**, *116*, 283.
6. Yuan, Z.; Wang, X.; Bin, J.; Peng, C.; Xing, S.; Wang, M.; Xiao, J.; Zeng, J.; Xie, Y.; Xiao, X. *Appl. Surf. Sci.* **2013**, *285*, 205.
7. Wang, R.; Hashimoto, K.; Fujishima, A.; Chikuni, M.; Kojima, E.; Kitamura, A.; Shimohigoshi, M.; Watanabe, T. *Nature* **1997**, *388*, 431.
8. Cui, Y.; Paxson, A. T.; Smyth, K. M.; Varanasi, K. K. *Colloids Surf. A* **2012**, *394*, 8.
9. Tompkins, B. D.; Fisher, E. R. *J. Appl. Polym. Sci.* **2015**, *132*, 41978.
10. Nagel, J.; Bräuer, M.; Hupfer, B.; Grundke, K.; Schwarz, S.; Lehmann, D. *J. Appl. Polym. Sci.* **2004**, *93*, 1186.
11. Gilliam, M.; Yu, Q. *J. Appl. Polym. Sci.* **2007**, *105*, 360.
12. Zhang, L.; Yu, H.; Zhao, N.; Dang, Z. M.; Xu, J. *J. Appl. Polym. Sci.* **2014**, *131*, 41057.
13. Moeller, M.; Matyjaszewski, K. Polymer Science: A Comprehensive Reference, 10 Volume Set; Newnes: Waltham, MA, **2012**.
14. Wang, S.; Liu, J.; Lv, M.; Zeng, X. *Appl. Surf. Sci.* **2014**, *314*, 679.

15. Farmer, R. A Study of Crystallization in Bisphenol A Polycarbonate; Virginia Polytechnic Institute and State University: VA, USA, **2001**.
16. Brandrup, J.; Immergut, E. H.; Grulke, E. A.; Abe, A.; Bloch, D. R. Polymer Handbook; Wiley: New York, **1999**.
17. Paxson, A. Condensation Heat Transfer on Nanoengineered Surfaces; Massachusetts Institute of Technology: MA, USA, **2009**.
18. Sperling, L. H. Introduction to Physical Polymer Science; John Wiley & Sons: Hoboken, New Jersey, **2006**.
19. de Oliveira, F. L. O.; Leite, M. C. M.; Couto, L. O.; Correia, T. R. *Polym. Bull.* **2011**, *67*, 1045.
20. Aharoni, S. M.; Murthy, N. S. *Int. J. Polym. Mater.* **1998**, *42*, 275.
21. Sheldon, R.; Blakey, P. *Nature* **1962**, *195*, 172.
22. Liang, G. G.; Cook, W. D.; Sautereau, H. J.; Tcharkhtchi, A. *Eur. Polym. J.* **2008**, *44*, 366.
23. Turska, E.; Przygocki, W.; Maslowski, M. *J. Polym. Sci. Part C: Polym. Symp.* **1968**, 3373.
24. Mercier, J.; Groeninckx, G.; Lesne, M. *J. Polym. Sci. Part C: Polym. Symp.* **1967**, *16*, 2059.
25. Turska, E.; Janeczek, H. *Polymer* **1979**, *20*, 855.
26. Yilbas, B.; Khaled, M.; Abu-Dheir, N.; Al-Aqeeli, N.; Said, S.; Ahmed, A.; Varanasi, K.; Toumi, Y. *Appl. Surf. Sci.* **2014**, *320*, 21.
27. Nakajima, A.; Hashimoto, K.; Watanabe, T.; Takai, K.; Yamauchi, G.; Fujishima, A. *Langmuir* **2000**, *16*, 7044.
28. Shirtcliffe, N. J.; McHale, G.; Atherton, S.; Newton, M. I. *Adv. Colloid Interface Sci.* **2010**, *161*, 124.
29. Bruynooghe, S.; Spinzig, S.; Fliedner, M.; Hsu, G. *Vakuum Forschung Und Praxis* **2008**, *20*, 25.
30. Wang, H.; Liu, Z.; Wang, E.; Yuan, R.; Gao, D.; Zhang, X.; Zhu, Y. *Appl. Surf. Sci.* **2015**, *332*, 518.
31. Liu, C. K.; Hu, C. T.; Lee, S. *Polym. Eng. Sci.* **2005**, *45*, 687.
32. Horcas, I.; Fernandez, R.; Gomez-Rodriguez, J.; Colchero, J.; Gómez-Herrero, J.; Baro, A. *Rev. Sci. Instrum.* **2007**, *78*, 013705.
33. Fan, Z.; Shu, C.; Yu, Y.; Zaporojtchenko, V.; Faupel, F. *Polym. Eng. Sci.* **2006**, *46*, 729.
34. Sinha, A.; De, P. Mass Transfer: Principles and Operations; PHI Learning Pvt. Ltd: New Delhi, India, **2012**.
35. Pandis, S. A. Atmospheric Chemistry and Physics, 2 ed.; John Wiley & Sons: Hoboken, New Jersey, **2006**.
36. Cassie, A.; Baxter, S. *Transactions of the Faraday Society* **1944**, *40*, 546.
37. Wenzel, R. N. *Ind. Eng. Chem.* **1936**, *28*, 988.
38. Xu, J.; Guo, B. H.; Yang, R.; Wu, Q.; Chen, G. Q.; Zhang, Z. M. *Polymer* **2002**, *43*, 6893.
39. Atkins, P.; Paula, J. Atkins' physical chemistry; Oxford, New York: Oxford University Press: **2012**.
40. Paragkumar N, T.; Edith, D.; Six, J. L. *Appl. Surf. Sci.* **2006**, *253*, 2758.
41. Ahmed, A. O. M. Design and fabrication of different textured surfaces with improved hydrophobicity for photovoltaic cells' applications; King Fahd University of Petroleum and Minerals: Dhahran, Saudi Arabia, **2014**.
42. Henke, B. L.; Gullikson, E. M.; Davis, J. C. *Atomic Data Nuclear Data Tables* **1993**, *54*, 181.